

# FusB energises import across the outer membrane through direct interaction with its ferredoxin substrate

Marta Wojnowska and Daniel Walker

Institute of Infection, Immunity and Inflammation, College of Medical, Veterinary and Life Sciences, University of Glasgow, Glasgow, G12 8QQ, UK.

Corresponding author: Daniel Walker, E-mail: [daniel.walker@glasgow.ac.uk](mailto:daniel.walker@glasgow.ac.uk)

**Abbreviations:** Ara – Arabidopsis, CCCP – carbonyl cyanide chlorophenylhydrazone, CTD – C-terminal domain, Fer - ferredoxin, GFP – green fluorescent protein, ITC – isothermal titration calorimetry, IUTD - intrinsically unstructured translocation domain, NTR – N-terminal region, , Pc – *Pectobacterium carotovorum*, PMF – proton motive force, Pot – potato, IPTG – isopropyl  $\beta$ -D-1 thiogalactopyranoside, SEC – size exclusion chromatography, Sp - spinach, TBDT – TonB-dependent transporter.

## Abstract

Phytopathogenic *Pectobacterium* spp. import ferredoxin into the periplasm for proteolytic processing and iron release via the ferredoxin uptake system. Although the ferredoxin receptor FusA and the processing protease, FusC, have been identified, the mechanistic basis of ferredoxin import is poorly understood. In this work we demonstrate that protein translocation across the outer membrane is dependent on the TonB-like protein FusB. In contrast to the loss of FusC, loss of FusB or FusA abolishes ferredoxin transport to the periplasm, demonstrating that FusA and FusB work in concert to transport ferredoxin across the outer membrane. In addition to interaction with the TonB-box region of FusA, FusB also forms a complex with the ferredoxin substrate, with complex formation required for substrate transport. These data suggest that ferredoxin transport requires energy transduction from the cytoplasmic membrane via FusB for both removal of the FusA plug domain and for substrate translocation through the FusA barrel.

## Introduction

Gram-negative bacteria have evolved a number of strategies for the acquisition of iron and other nutrients in which TonB-dependent transporters (TBDTs) play a central role<sup>1</sup>. In the case of siderophore-mediated iron acquisition the iron-siderophore complex is imported into the cell, captured by a siderophore-specific periplasmic binding protein and delivered to an ABC-transporter for import to the cytoplasm<sup>2</sup>. For iron acquisition from large host proteins such as transferrin, the iron-containing protein is captured at the cell surface through TBDT binding and the iron stripped at the cell surface and subsequently transported through the lumen of the TBDT<sup>3</sup>. In addition to the outer membrane receptor, whose lumen constitutes the translocation route, TBDT-mediated transport requires a complex of three proteins anchored in the inner membrane: TonB, ExbB and ExbD<sup>4,5</sup>. The ExbBD-TonB complex allows the entry of the nutrient by removal of a force-labile portion of the plug domain, which obstructs the receptor lumen<sup>6</sup>. ExbB and ExbD are related to the flagellar motor proteins and harness proton motive force to energise the transport process.

In addition to the uptake of iron siderophores and other metal chelating compounds such as vitamin B<sub>12</sub>, TBDTs also transport complex carbohydrates and simple sugars<sup>7</sup>. A recent study has also described the role of a TonB-dependent receptor in protein export, suggesting that TonB-dependent receptors are highly adaptable to the transport of diverse substrates across the OM<sup>8</sup>. The flexibility in the range of substrates that are amenable to transport by TBDTs is exploited by protein antibiotics such as colicins and pyocins that use TBDTs as their primary cell surface receptor and translocator<sup>9</sup>. As with the uptake of nutrients, translocation of colicins and pyocins via TBDTs is PMF-dependent, although in these cases the periplasm-spanning protein TonB is required both to remove the force labile region of the TBDT-plug domain and to subsequently energise protein translocation across the OM<sup>10</sup>. Protein translocation occurs by direct interaction with the an N-terminal intrinsically unstructured region of the toxin that, similar to the TBDTs, carries a TonB-binding motif<sup>10</sup>.

We recently demonstrated that TBDT-mediated iron acquisition from the iron-sulphur cluster containing protein ferredoxin represents an unprecedented example of protein translocation into the bacterial cell for nutrient acquisition<sup>11</sup>. Ferredoxin binding at the cell surface is mediated by the TBDT FusA and, following transport of intact ferredoxin into the periplasm, the substrate is subjected to proteolytic processing by the M16 protease FusC<sup>11,12</sup>. Cleavage by FusC results in release of the iron-sulphur cluster and is required for effective iron acquisition from ferredoxin by *Pectobacterium*. Together with the genes encoding FusA and FusC, the Fus operon contains two additional genes, with *fusB* encoding a TonB-homologue and *fusD* a putative ABC transporter<sup>12</sup>. Interestingly, the M-type pectocins M1 and M2, which we have previously described, parasitise the ferredoxin uptake

system through an N-terminal ferredoxin domain that is highly homologous to plant ferredoxins<sup>13,14</sup>.

More recently, the X-ray structure of FusC bound to ferredoxin has been reported, showing that substrate recognition occurs at a site distant from the active site<sup>15</sup>. Furthermore, only parts of the ferredoxin molecule are visible in the structure, implying that the bound substrate is largely unstructured. Based on these data, it was suggested that ferredoxin transport occurs by means of a Brownian ratchet mechanism in which FusC acts as a periplasmic anchor to facilitate translocation of ferredoxin across the OM via the lumen of FusA<sup>12,15</sup>. Similar mechanisms have been postulated to account for mitochondrial protein uptake, whereby cytoplasmically synthesised proteins are translocated via the TOM and TIM23 complexes<sup>16,17</sup>. As such, this would represent a hitherto unexpected evolutionary link between mitochondrial and plastid protein import and bacterial protein import via the Fus and other postulated protein uptake systems.

In this work we show that FusC does not facilitate ferredoxin import and that like the import of other TBDT substrates, ferredoxin uptake is PMF-dependent. Instead, we show that the TonB-homologue encoded within the *fus* operon, FusB, is required for ferredoxin import and the mechanism of ferredoxin import involves a direct interaction between FusB and the ferredoxin substrate. The direct interaction of the TonB-like protein with substrate is unprecedented and explains the requirement for the system-specific TonB-homologue in the Fus system. Our data also show that, in addition to the direct interaction with the substrate, FusB fulfils another role - similar to other TonB proteins - in interacting with the TonB-box of FusA for plug displacement. Since multiple genes encoding TonB-like proteins are commonly found in the genomes of Gram-negative bacteria this may be a common mechanism for the uptake of atypical substrates via TonB-dependent receptors.

## Results

### ***Ferredoxin import is independent of FusC but requires proton motive force***

We previously showed that FusC is a highly specific protease that targets plant ferredoxin to release iron from this host protein in the periplasm of *Pectobacterium* spp<sup>11</sup>. However, it has also been suggested that FusC plays an additional role in iron acquisition through a direct involvement in ferredoxin transport across the outer membrane by means of a Brownian ratchet mechanism, specifically acting as a periplasmic anchor<sup>15</sup>. Our own previous work suggests that if FusC does play a role in ferredoxin import this role is not essential since the accumulation of Arabidopsis ferredoxin can still be observed in a *P. carotovorum* LMG2410 (*Pc*LMG2410) strain lacking FusC<sup>11</sup>. However, using Arabidopsis ferredoxin ( $\text{Fer}_{\text{Ara}}$ ) it is not possible to directly compare the rate and extent of ferredoxin uptake between wild-type and  $\Delta fusC$  *P. carotovorum* since  $\text{Fer}_{\text{Ara}}$  is cleaved by FusC on import to the periplasm in the wild-type strain; hence, based on these data, we could not rule out a role for FusC in ferredoxin import.

To test the hypothesis that FusC facilitates translocation of ferredoxin to the periplasm we compared the uptake of potato ferredoxin ( $\text{Fer}_{\text{Pot}}$ ) in wild-type and  $\Delta fusC$  *Pc*LMG2410.  $\text{Fer}_{\text{Pot}}$  was used as we had observed that, although similarly to  $\text{Fer}_{\text{Ara}}$ , it can be transported into cells (Figure 1a), unlike  $\text{Fer}_{\text{Ara}}$  and spinach ferredoxin ( $\text{Fer}_{\text{Sp}}$ ), which both support robust growth of *Pc*LMG2410 under iron-limiting conditions<sup>12,13</sup>, it is not cleaved at an appreciable rate by FusC and so accumulates intracellularly in wild-type *Pc*LMG2410 (Figure 1b). To compare uptake of  $\text{Fer}_{\text{Pot}}$  in wild-type and  $\Delta fusC$  *Pc*LMG2410, cells were grown under iron-limiting conditions through the addition of the iron chelator, 2,2'-bipyridine, and supplemented with  $\text{Fer}_{\text{Pot}}$ . The amount of  $\text{Fer}_{\text{Pot}}$  in whole cell extracts and the media was determined by immunoblotting. Levels of  $\text{Fer}_{\text{Pot}}$  obtained from cell extracts increased at the same rate in whole cell extracts and rates of removal of ferredoxin from the media were similar (Figure 1c). These data show that FusC does not play a role in protein import and the role of FusC in iron acquisition is likely restricted to proteolytic processing of ferredoxin as we previously reported<sup>11</sup>.

To further probe the mechanism of ferredoxin uptake we tested the ability of *Pc*LMG2410 cells to accumulate  $\text{Fer}_{\text{Pot}}$  under iron-limiting conditions and in the presence of the uncoupling agent carbonyl cyanide m-chlorophenylhydrazone (CCCP), which dissipates the PMF through transport of protons across the cytoplasmic membrane<sup>18</sup>. The intracellular accumulation of  $\text{Fer}_{\text{Pot}}$  by *Pc*LMG2410 was markedly reduced in the presence of 10  $\mu\text{M}$  CCCP, relative to cells grown in the absence of the uncoupling agent, and abolished at 100  $\mu\text{M}$  CCCP (Figure 1d). Similar effects through the action of CCCP were observed on the intracellular accumulation of Arabidopsis ferredoxin by  $\Delta fusC$  LMG2410 (Figure 1d). These data show that, analogously to other TBDT-mediated transport processes<sup>10,19</sup>, the import of

ferredoxin is PMF-dependent and a Brownian ratchet mechanism is unlikely to play a key role in ferredoxin import in *Pectobacterium* spp.

### ***FusB* mediates ferredoxin import into the periplasm**

As we previously reported, in addition to *fusA* and *fusC*, the *Fus* operon carries additional genes that encode a TonB homologue, *FusB*, and an ABC transporter *FusD*<sup>12</sup>. Given the documented role of TonB in siderophore import in many bacterial species we supposed *FusB* may play a similar role in protein import, having perhaps evolved additional functionality required to mediate the passage of a large substrate through the lumen of the TBDT *FusA*. To test this hypothesis we created  $\Delta fusA$  and  $\Delta fusB$  strains in *Pc*LMG2410 and initially probed them using growth enhancement assays under iron-limiting conditions. As indicated by the loss of growth enhancement both on solid media (Figure 2a) and in liquid culture (Figure 2b), these two genes encode proteins which are essential for *Fus*-mediated iron acquisition. The possibility that deletion of either gene affected the expression or level of *FusC*, thus indirectly affecting the growth enhancement phenotype, was ruled out by immunoblotting whole cell extracts with anti-*FusC* antiserum (Figure S1). We further investigated the ability of the  $\Delta fusA$  and  $\Delta fusB$  *Pc*LMG2410 to import ferredoxin relative to wild-type and  $\Delta fusC$  strains using  $Fer_{Pot}$ , which cannot be cleaved by *FusC*. Consistent with the hypothesised role of *FusB* in protein import, and in contrast to wild-type and  $\Delta fusC$  strains, we did not observe the intracellular accumulation of  $Fer_{Pot}$  in  $\Delta fusA$  and  $\Delta fusB$  *Pc*LMG2410 (Figure 2c). The ferredoxin import phenotype lost in the  $\Delta fusA$  and  $\Delta fusB$  strains was restored by plasmid-based complementation of *fusA* and *fusB*, respectively (Figure 2d). In these experiments the production of *FusA* and *FusB* is IPTG-inducible under the control of the T5 promoter, although in the case of *FusB* complementation, leaky expression in the absence of IPTG is sufficient to restore protein import.

To ensure that the abrogation of substrate import is not specific to  $Fer_{Pot}$  we also monitored the ability of the  $\Delta fusA$  and  $\Delta fusB$  strains to utilise  $Fer_{Ara}$ . However, for this substrate instead of measuring intracellular ferredoxin accumulation, we determined loss of ferredoxin from the growth media, since accumulation of  $Fer_{Ara}$  is only observed in the LMG2410  $\Delta fusC$  strain (Figure 2e). Consistent with the internalisation assay and growth enhancement assays, ferredoxin content of the media decreased over time in the presence of wild type cells, but not in the presence of the  $\Delta fusA$  and  $\Delta fusB$  strains, indicating that both *FusA* and *FusB* are required for  $Fer_{Ara}$  uptake (Figure 2f).

### ***FusB* directly interacts with the 'TonB-box' of *FusA***

Having determined that the TonB-like protein FusB is required for ferredoxin import we aimed to elucidate the mechanism of ferredoxin uptake. Analysis of the FusA sequence showed the presence of a putative TonB-box, DTILVRST, with a similar sequence to TonB-boxes from well-characterised *E. coli* TBDTs and other *PcLMG2410* TBDTs (Figure S2). The functional importance of this putative TonB-box region was demonstrated using ferredoxin import assay and plasmid-based complementation of the  $\Delta fusA$  strain, which showed that proline substitutions within the putative TonB-box abolish internalisation of the FusA substrate ferredoxin (Figure S3). The similarity of the TonB-box of FusA to the TonB-boxes of other *PcLMG2410* and *E. coli* TBDTs suggests that FusA may interact with *PcLMG2410* TonB and not FusB. Although *PcLMG2410* has 6 genes that encode TonB-like proteins, we hypothesised that the protein that was most similar to *E. coli* TonB, which we refer to as *PcTonB*, would fulfil the same function as this protein in servicing multiple TBDTs, with the primary function of dislocating the plug domain to enable substrate transport.

To determine if TonB and/or FusB interact directly with FusA we produced a construct consisting of the N-terminal region of FusA (residues 21 to 66), excluding the signal peptide region, fused to GFP (FusA<sub>NTR</sub>-GFP) and determined if this interacts with the isolated C-terminal domains of *PcTonB* (TonB<sub>CTD</sub>) and FusB (FusB<sub>CTD</sub>) by ITC. Clear heats of binding were observed on titration of FusA<sub>NTR</sub>-GFP into FusB<sub>CTD</sub>, although the affinity of FusB<sub>CTD</sub> for FusA<sub>NTR</sub>-GFP is weak (57  $\mu$ M) (Figure 3a). No heats of binding were observed on titration of isolated GFP into FusB<sub>CTD</sub>, (Figure S4) showing that the C-terminal domain of FusB specifically interacts with the N-terminal region of FusA. Interestingly, similar heats of binding were observed on titration of FusA<sub>NTR</sub>-GFP into TonB<sub>CTD</sub> (Figure S5), demonstrating that the N-terminal region of FusA can also interact with *PcTonB*.

To determine if the *PcTonB* plays a role in ferredoxin uptake, we deleted the respective gene in *PcLMG2410* and tested the growth enhancement phenotype of this strain in the presence of Fer<sub>Sp</sub>. In contrast to deletion of *fusB*, the loss of *tonB* did not reduce growth enhancement phenotype (Figure 3b); in fact, the  $\Delta tonB$  strain showed more prominent zones of growth enhancement in the presence of Fer<sub>Sp</sub> relative to the wild-type strain and showed increased intracellular accumulation of Fer<sub>Pot</sub> relative to wild-type *PcLMG2410* (Figure 3c). However, *PcLMG2410*  $\Delta tonB$  exhibited poor growth in the presence of 2,2'-bipyridine relative to the wild-type strain (Figure 3d), with very faint growth observable after 24 hours. These data indicate that, although *PcTonB* does play the expected generic role in iron uptake, this does not include iron acquisition from ferredoxin. Furthermore, despite the aforementioned observation that TonB interacts with FusA *in vitro* (and possibly *in vivo*), this interaction is not sufficient for ferredoxin uptake. Indeed there may be competition between FusB and TonB for complex formation with FusA, with only the FusB-FusA complex being productive with respect to ferredoxin uptake.

### ***FusB interacts directly with the ferredoxin substrate***

The ability of FusB and *PcTonB* to interact with FusA, but with only the former able to mediate ferredoxin uptake, suggests that FusB plays an additional role, which is essential for ferredoxin import. One possibility is that FusB directly interacts with the protein substrate after the initial binding of ferredoxin to FusA at the cell surface. To test this, we sought to determine if ferredoxin forms a complex with the isolated C-terminal domain of FusB by size exclusion chromatography (SEC). SEC of ferredoxin mixed with FusB<sub>CTD</sub> monitored at 280 nm and 330 nm gave a peak indicating the presence of a species of higher molecular weight than FusB<sub>CTD</sub> or Fer<sub>SP</sub> alone, providing evidence of complex formation (Figure 4a). In contrast, no complex formation was observed between ferredoxin and the purified C-terminal domain of TonB (TonB<sub>CTD</sub>) using SEC (Figure S6). We further investigated the formation of the FusB<sub>CTD</sub>-Fer<sub>SP</sub> complex by isothermal titration calorimetry, titrating Fer<sub>SP</sub> into FusB<sub>CTD</sub> (Figure 4b). These data show that FusB interacts directly with the ferredoxin substrate.

Inspection of the amino acid sequence of FusB shows that the N-terminal portion of the predicted globular domain and the preceding linker contain a significant number of positively charged amino acids, which are absent from *PcLMG2410* and *E. coli* TonBs (Figure S7). Two such residues (Arg176, Arg177) are found in place of the highly conserved Gln-Pro-Gln residues, which form a part of the BtuB TonB-box binding motif (QPQYP) in *E. coli* TonB<sup>20</sup>. This arginine motif is located within a loop/linker region of TonBs, connecting the periplasmic-spanning and globular domains. Substitution of the two FusB<sub>CTD</sub> arginine residues with lysines rendered a folded protein that did not comigrate with ferredoxin in gel filtration or interact with the substrate in ITC experiments (Figure S8). Similarly, *PcLMG2410*  $\Delta fusB$  could not be complemented with a pFusB plasmid encoding the FusB R176K/R177K variant (Figure 4c). Therefore at least one of these two arginine residues appears to be critical for FusB-substrate interaction.



## Discussion

Our recent discovery that ferredoxin is imported into the periplasm of *P. carotovorum* revealed an unprecedented example of protein uptake for nutrient acquisition in Gram-negative bacteria<sup>11</sup>. In this work, we define key aspects of the mechanism of ferredoxin transport across the outer membrane. In a recent report, it was hypothesised that the M16 protease FusC acts as a periplasmic anchor that facilitates ferredoxin uptake by means of Brownian-ratchet mechanism<sup>15</sup>. However, the data presented here are inconsistent with this model, showing that ferredoxin import is independent of FusC. Instead, ferredoxin uptake requires energy transduction from the PMF and the TonB-like protein FusB. Therefore, the mechanism of ferredoxin import shares some similarity with the mechanism of import of widely studied substrates of TBDRs, such iron siderophores and vitamin B<sub>12</sub><sup>4,21</sup>. For these substrates, according to the currently accepted models of TonB-dependent transport, the major role of TonB is in the displacement or partial displacement of the plug domain from their specific TBDTs<sup>6,10</sup>.

Interestingly, in the case of FusA, both FusB and *Pc*TonB are able to interact with its N-terminal region and so both these proteins may be able to facilitate displacement of the FusA plug domain. However, deletion of the genes encoding the two TonB proteins showed that only FusB is essential for ferredoxin transport, demonstrating an additional role for FusB in this process that cannot be fulfilled by *Pc*TonB. Although the affinity of FusB<sub>CTD</sub> for FusA<sub>NTR</sub> is low (57  $\mu$ M), comparable low affinity complexes have been described between TBDT TonB-binding peptides and TonB proteins. For example, the affinity reported for the TonB-like protein HasB interaction with 21-mer HasR N-terminal peptide is 25  $\mu$ M<sup>22</sup>. Similarly weak interactions between TonB and TBDR TonB-box peptides have been reported for FhuA (36  $\mu$ M)<sup>23</sup> and BtuB (9.4  $\mu$ M)<sup>6</sup>. However, complex formation between TonB and TonB-binding peptides is characterised by  $\beta$ -strand augmentation which is known to result in the formation of mechanically strong complexes<sup>6</sup>. Indeed, it has been demonstrated *in vitro* using atomic force microscopy that the TonB–BtuB Ton box complex is sufficiently mechanically robust to induce partial unfolding of the BtuB plug-domain, forming a channel through which the vitamin B<sub>12</sub> substrate can translocate<sup>6</sup>.

The ability of FusB to form a complex with ferredoxin, which *Pc*TonB lacks, indicates that this additional role involves the direct interaction of FusB with the ferredoxin substrate and that this complex formation is essential for ferredoxin transport through the lumen of FusA. Consistent with this, we identified an arginine motif that is required for FusB-mediated ferredoxin uptake by *P. carotovorum* and formation of the FusB-ferredoxin complex. Our current model of Fus-mediated iron acquisition, whereby FusB fulfils two distinct roles, is schematically shown in Figure 5. In this model, binding of the substrate on the extracellular side of FusA releases the TonB-box into the periplasmic space, where it is captured by

FusB. Due to the dimensions of the globular ferredoxin, which are similar to the lumen of its FusA TBDT<sup>11</sup>, ferredoxin is unlikely to be able to readily diffuse into the periplasm after removal of the FusA plug domain. We therefore hypothesise that the interaction of FusB with the substrate involves a further PMF dependent step required to pull the ferredoxin substrate through the lumen of FusA. This would involve the C-terminal domain of FusB, which is of comparable size to plant ferredoxins, to enter the lumen of FusA to contact ferredoxin on the cell surface. The FusB-ferredoxin complex can then be pulled into the periplasm, using the ExbBD complex and PMF, after which the substrate is processed by FusC. Although we present a model relying on a single FusB per import cycle, we cannot exclude the possibility that the removal of FusA plug and ferredoxin import would involve two separate FusB molecules.

The occurrence of genes encoding multiple TonB-like proteins is a common feature of many Gram-negative bacteria<sup>24</sup> and in some cases specific TonB proteins are required for the uptake of specific substrates, as for TonB2 of *Vibrio anguillarum* for anguibactin uptake<sup>25</sup>, while others exhibit some level of functional redundancy<sup>26</sup>. However, to our knowledge the Fus system represents the only substrate import system in which a TonB protein has been shown to directly interact with the substrate. This additional functionality displayed by FusB may reflect the nature of the ferredoxin substrate, which is atypically large in comparison to the well-studied TBDT siderophore substrates. In this respect, the uptake of ferredoxin is similar to the TonB-dependent uptake of the colicins and pyocins, which directly interact with TonB after threading their TonB box-containing intrinsically unstructured translocation domain (IUTD) through the lumen of their respective TBDT<sup>10,27</sup>. However, since plant ferredoxins are highly stable proteins that lack any kind of similar unstructured regions, our hypothesis is that in order to contact ferredoxin, FusB must enter the FusA lumen and contact FusA-bound substrate at the cell surface. This proposed mechanism also accounts for why the ferredoxin-containing bacteriocins do not require an IUTD that contains a TonB-box to cross the *P. carotovorum* outer membrane, with FusB able to directly contact their ferredoxin receptor-binding domains at the cell surface, thus enabling parasitisation of the Fus system<sup>12,28</sup>.

In summary, we describe a novel mechanism of 'TonB-dependent' nutrient uptake that requires a direct interaction between substrate and cognate TonB protein. The occurrence of multiple TonB proteins in many Gram-negative bacteria suggests that similar mechanisms may operate for atypical TBDT substrates.

## Material and Methods

### *Bacterial strains and media*

*E. coli* was grown in LB broth or plated on LB agar and grown at 37 °C. DH5 $\alpha$  and BL21 (DE3) strains were used as host strains for cloning and for IPTG-induced protein expression, respectively. *P. carotovorum* was grown in LB broth or plated on LB agar at 30°C with the addition of the iron chelator 2,2'-bipyridine where specified. LB media and agar for culturing plasmid-complemented deletion strains always contained 100  $\mu\text{g ml}^{-1}$  ampicillin.

### *Generation of gene knockout strains and plasmids*

The *fusA* (KAA3668913), *fusB* (KAA3668912), *fusC* (KAA3668914) and *tonB* (KAA3668374) sequences were determined from the genome sequence of *P. carotovorum* LMG2410 (GenBank: BioProject PRJNA543207)<sup>29</sup>. Genes in of *Pc*LMG2410 were deleted using the lambda red method as described previously<sup>11,30</sup>. The primers used for amplifying the kanamycin cassette from pKD4 template plasmid, gene sequences from genomic DNA and plasmid site-directed mutagenesis are listed in Table S1. The gene knockouts were confirmed by PCR and sequencing. Table S2 shows all the plasmids used in this study. To construct all plasmids, except pFusANTR-GFP, the respective genes were amplified from wild-type genomic DNA using primers that contained flanking regions with NdeI (forward) and XhoI (reverse) restriction enzyme sites. Purified PCR products were digested and ligated into NdeI/XhoI-digested pJ404, which carries ampicillin resistance. To generate pFusANTR-GFP the sequence encoding the N-terminal portion of FusA was amplified with primers containing XhoI (forward) and BamHI (reverse) restriction enzyme sites and the PCR products were inserted into XhoI/BamHI-digested pWaldo plasmid (Waldo et al 1999). The complementation plasmids were transformed into competent LMG2410 knockout strains by electroporation.

### *Protein production and purification*

FusC, FusB<sub>CTD</sub>, TonB<sub>CTD</sub>, FusA<sub>NTR</sub>-GFP and all ferredoxin proteins were overproduced in *E. coli* and purified as described previously<sup>11,12</sup>, except spinach ferredoxin (Fer<sub>Sp</sub>) which was purchased from Sigma. GFP alone used as a negative control in ITC was produced by cleavage of FusA<sub>NTR</sub>-GFP with TEV protease for 2 hours at RT, at 50:1 ratio. The resulting GFP-His<sub>8</sub> was separated from residual TEV protease by size-exclusion chromatography and the removal of the N-terminal region of FusA was confirmed by SDS PAGE.

### *Growth enhancement assays*

Growth enhancement in the presence of ferredoxin was performed on solid media as previously described<sup>11</sup>. Briefly, 10 ml of 0.8% pre-cooled agar was supplemented with 50  $\mu$ l of mid-log culture in LB media and poured onto an LB agar base containing 400  $\mu$ M 2,2'-bipyridine (and 0.2 mM IPTG where specified). For plasmid based complementation, 100  $\mu$ g/ml ampicillin was added to the LB media base. 4  $\mu$ l of ferredoxin at specified concentration was spotted onto the solidified plate. For growth enhancement in liquid media bacteria were grown in M9 minimal media. 10 ml cultures were inoculated with 1 in 50 dilution of overnight LB cultures and upon reaching OD<sub>600</sub>=0.45 they were supplemented with 0.2  $\mu$ M Fer<sub>Ara</sub> and growth was monitored by measuring the OD<sub>600</sub> for 6 hours.

### *Ferredoxin internalisation and depletion assays*

The time course of ferredoxin internalisation was initiated by supplementing LB cultures of wild type or  $\Delta fusC$  cells (OD<sub>600</sub>=0.5) with 2,2'-bipyridine to a final concentration of 200  $\mu$ M. Fer<sub>Ara</sub> or Fer<sub>Pot</sub> was added to a final concentration of 1  $\mu$ M and the cultures were grown at 30°C with shaking over the specified time. At each time point a volume equivalent to 1 ml cell suspension at OD<sub>600</sub>=0.5 was removed, the cells were spun down and treated with BugBuster (Merck) for soluble protein extraction. To determine if  $\Delta fusA$  and  $\Delta fusB$  strains can take up ferredoxin, LB cultures of WT and deletion strains at OD ~ 0.5 were supplemented with 200  $\mu$ M 2,2'-bipyridine and 1  $\mu$ M *Arabidopsis* or 5  $\mu$ M potato ferredoxin. After 2 hours at 30°C with shaking 1 ml of cells was pelleted and soluble proteins were extracted using BugBuster (Merck). For internalisation experiments involving plasmid-complemented deletion strains, LB cultures were grown until OD<sub>600</sub>=0.4 was reached, whereupon 2,2'-bipyridine and potato ferredoxin were added.  $\Delta fusA$ +pFusA and  $\Delta fusB$ +pFusB cultures were split into two separate tubes, one of which was supplemented with IPTG to a final concentration of 0.2 mM. After 2 hours cells were harvested and subjected to BugBuster extraction as described above.

Depletion of *Arabidopsis* ferredoxin was monitored in 2 ml M9 minimal media cultures of WT,  $\Delta fusA$  and  $\Delta fusB$  strains over the course of 4 hours. Each culture, as well as 2 ml of uninoculated media (negative control), was supplemented 100  $\mu$ M 2,2'-bipyridine and 1  $\mu$ M Fer<sub>Ara</sub>. At each time point 50  $\mu$ l of culture was removed from each tube and after pelleting the cells the supernatant was mixed with SDS loading dye.

The effect of dissipating PMF on ferredoxin uptake was determined using protonophore CCCP (Sigma), which was dissolved in DMSO to a final concentration of 10 mM. Mid-log cultures of wild type and  $\Delta fusC$  P<sub>c</sub>LMG2410 in M9 media were supplemented with 300  $\mu$ M 2,2'-bipyridine and 2 ml of each culture was mixed with 18  $\mu$ l DMSO and 2  $\mu$ l CCCP stock (for 10  $\mu$ M final CCCP concentration) or 20  $\mu$ l CCCP stock (10  $\mu$ M final CCCP

concentration) or 20  $\mu$ l DMSO for the “no CCCP” control. The cultures were mixed and incubated at room temperature for 10 min, after which wild type cultures were supplemented with 1  $\mu$ M Fer<sub>Pot</sub> and  $\Delta fusC$  cultures with 0.2  $\mu$ M Fer<sub>Ara</sub>. After 45 min incubation at 30°C with shaking, 1 ml of each culture was pelleted, washed with 0.5 ml PBS and subjected to BugBuster extraction.

#### *Ferredoxin cleavage assays*

Cleavage reactions were performed in 10 mM Tris-HCl, pH 7.5, 50 mM NaCl, with 2  $\mu$ M FusC and 250  $\mu$ M ferredoxin at RT. At each time point 12  $\mu$ l were removed and mixed with SDS loading dye. Proteins were resolved on a 16% SDS PAGE gel and visualised by Coomassie staining.

#### *Analytical size-exclusion chromatography*

Proteins were concentrated to ~600  $\mu$ M and 20  $\mu$ l of TonB<sub>CTD</sub> or the relevant construct of FusB<sub>CTD</sub> was mixed with an equal volume of Fer<sub>Sp</sub>. The mixtures were then diluted with SEC buffer (20 mM Tris-HCl, pH 7.5, 150 mM NaCl) to 0.2 ml and loaded onto Superdex 75 10/300 column (GE Healthcare), pre-equilibrated in the same buffer. Each protein was also passed through the column individually for reference. The chromatograms were recorded at both 280 and 330 nm.

#### *Isothermal titration calorimetry*

Experiments were performed on a MicroCal iTC<sub>200</sub> instrument (Malvern) at 25°C in 10 mM Tris-HCl pH 7.5, 150 mM NaCl, with differential power set to 3. All proteins were dialysed against the ITC buffer overnight at 4°C except FusB<sub>CTD</sub> and TonB<sub>CTD</sub>, which were passed through gel filtration in ITC buffer immediately before the experiment. Each type of titration was repeated at least once using different batches of purified proteins. 2  $\mu$ l injections were used and titrations were continued until the signal represented heats of dilution. The magnitude of heats of dilution for each titrant was established in a separate experiment, where the titrant was injected into buffer.  $K_d$  values are expressed as the mean ( $\pm$ SEM).

## References

1. Krewulak, K. D. & Vogel, H. J. TonB or not TonB: is that the question? *Biochem. Cell Biol.* **89**, 87–97 (2011).
2. Noinaj, N., Guillier, M., Barnard, T. J. & Buchanan, S. K. TonB-dependent transporters: regulation, structure, and function. *Annu. Rev. Microbiol.* **64**, 43–60 (2010).
3. Noinaj, N. *et al.* Structural basis for iron piracy by pathogenic *Neisseria*. *Nature* **483**, 53–58 (2012).
4. Celia, H. *et al.* Structural insight into the role of the Ton complex in energy transduction. *Nature* **538**, 60–65 (2016).
5. Maki-Yonekura, S. *et al.* Hexameric and pentameric complexes of the ExbBD energizer in the Ton system. *Elife* **7**, (2018).
6. Hickman, S. J., Cooper, R. E. M., Bellucci, L., Paci, E. & Brockwell, D. J. Gating of TonB-dependent transporters by substrate-specific forced remodelling. *Nat. Commun.* **8**, 14804 (2017).
7. Glenwright, A. J. *et al.* Structural basis for nutrient acquisition by dominant members of the human gut microbiota. *Nature* **541**, 407–411 (2017).
8. Gómez-Santos, N., Glatter, T., Koebnik, R., Świątek-Połatyńska, M. A. & Søgaard-Andersen, L. A TonB-dependent transporter is required for secretion of protease PopC across the bacterial outer membrane. *Nat. Commun.* **10**, 1360 (2019).
9. Kleanthous, C. Swimming against the tide: progress and challenges in our understanding of colicin translocation. *Nat. Rev. Microbiol.* **8**, 843–848 (2010).
10. White, P. *et al.* Exploitation of an iron transporter for bacterial protein antibiotic import. *Proc. Natl. Acad. Sci.* **114**, 12051–12056 (2017).
11. Mosbahi, K., Wojnowska, M., Albalat, A. & Walker, D. Bacterial iron acquisition mediated by outer membrane translocation and cleavage of a host protein. *Proc. Natl. Acad. Sci. U. S. A.* **115**, 6840–6845 (2018).
12. Grinter, R. *et al.* Structure of the bacterial plant-ferredoxin receptor FusA. *Nat. Commun.* **7**, (2016).
13. Grinter, R., Milner, J. & Walker, D. Ferredoxin Containing Bacteriocins Suggest a Novel Mechanism of Iron Uptake in *Pectobacterium* spp. *PLoS One* **7**, e33033 (2012).

14. Grinter, R. *et al.* Structure of the atypical bacteriocin pectocin M2 implies a novel mechanism of protein uptake. *Mol. Microbiol.* **93**, 234–46 (2014).
15. Grinter, R. *et al.* FusC, a member of the M16 protease family acquired by bacteria for iron piracy against plants. *PLOS Biol.* **16**, e2006026 (2018).
16. Neupert, W. & Brunner, M. The protein import motor of mitochondria. *Nat. Rev. Mol. Cell Biol.* **3**, 555–565 (2002).
17. Backes, S. & Herrmann, J. M. Protein Translocation into the Intermembrane Space and Matrix of Mitochondria: Mechanisms and Driving Forces. *Front. Mol. Biosci.* **4**, 83 (2017).
18. Kasianowicz, J., Benz, R. & McLaughlin, S. The kinetic mechanism by which CCCP (carbonyl cyanidem-Chlorophenylhydrazone) transports protons across membranes. *J. Membr. Biol.* **82**, 179–190 (1984).
19. Braud, A., Hannauer, M., Mislin, G. L. A. & Schalk, I. J. The *Pseudomonas aeruginosa* pyochelin-iron uptake pathway and its metal specificity. *J. Bacteriol.* **191**, 3517–25 (2009).
20. Shultis, D. D., Purdy, M. D., Banchs, C. N. & Wiener, M. C. Outer membrane active transport: structure of the BtuB:TonB complex. *Science* **312**, 1396–9 (2006).
21. Ferguson, A. D. *et al.* Structural basis of gating by the outer membrane transporter FecA. *Science* **295**, 1715–9 (2002).
22. Amorim, G. C. de *et al.* The Structure of HasB Reveals a New Class of TonB Protein Fold. *PLoS One* **8**, e58964 (2013).
23. Sean Peacock, R., Weljie, A. M., Peter Howard, S., Price, F. D. & Vogel, H. J. The solution structure of the C-terminal domain of TonB and interaction studies with TonB box peptides. *J. Mol. Biol.* **345**, 1185–1197 (2005).
24. Schauer, K., Rodionov, D. A. & de Reuse, H. New substrates for TonB-dependent transport: do we only see the ‘tip of the iceberg’? *Trends Biochem. Sci.* **33**, 330–8 (2008).
25. López, C. S., Peacock, R. S., Crosa, J. H. & Vogel, H. J. Molecular characterization of the TonB2 protein from the fish pathogen *Vibrio anguillarum*. *Biochem. J.* **418**, 49–59 (2009).
26. Paquelin, A., Ghigo, J. M., Bertin, S. & Wandersman, C. Characterization of HasB, a *Serratia marcescens* TonB-like protein specifically involved in the haemophore-

- dependent haem acquisition system. *Mol. Microbiol.* **42**, 995–1005 (2001).
27. Cascales, E. *et al.* Colicin Biology. *Microbiol. Mol. Biol. Rev.* **71**, 158–229 (2007).
  28. Grinter, R. *et al.* Structure of the atypical bacteriocin pectocin M2 implies a novel mechanism of protein uptake. *Mol. Microbiol.* **93**, (2014).
  29. Rooney, W. M., Wojnowska, M. & Walker, D. Draft Genome Sequence of the Necrotrophic Plant-Pathogenic Bacterium *Pectobacterium carotovorum* subsp. *carotovorum* Strain LMG 2410. *Microbiol. Resour. Announc.* **8**, e00614-19 (2019).
  30. Datsenko, K. A. & Wanner, B. L. One-step inactivation of chromosomal genes in *Escherichia coli* K-12 using PCR products. *Proc. Natl. Acad. Sci.* **97**, 6640–6645 (2000).



## Figure Legends

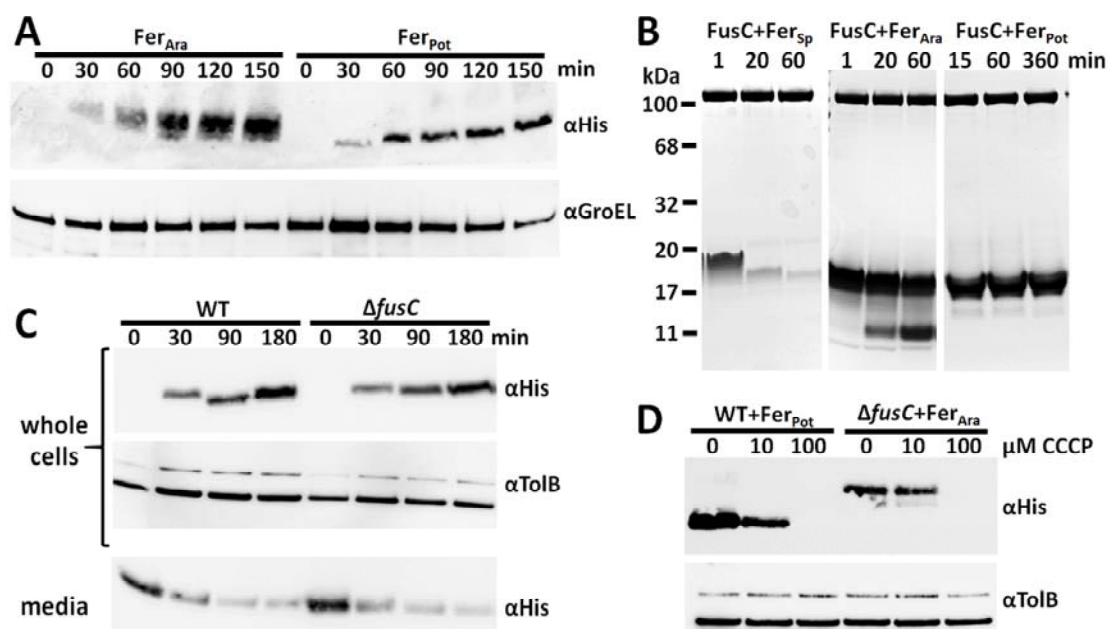


**Figure 1. Import of ferredoxin is FusC-independent and requires proton motive force.**

(A) Uptake of Fer<sub>Ara</sub> and Fer<sub>Pot</sub> by  $\Delta fusC$  cells over time determined by immunoblotting of whole cell extracts; GroEL serves as loading control. (B) FusC-mediated cleavage assays of plant ferredoxins. (C) Comparison of Fer<sub>Pot</sub> uptake by wild-type (WT) and  $\Delta fusC$  cells with TolB as the loading control; the bottom panel showing the concomitant depletion of ferredoxin from the media. (D) Ferredoxin import assays in the presence of protonophore CCCP; Fer<sub>Pot</sub> was used as a reporter in wild type cells while Fer<sub>Ara</sub> was used in  $\Delta fusC$  cells.

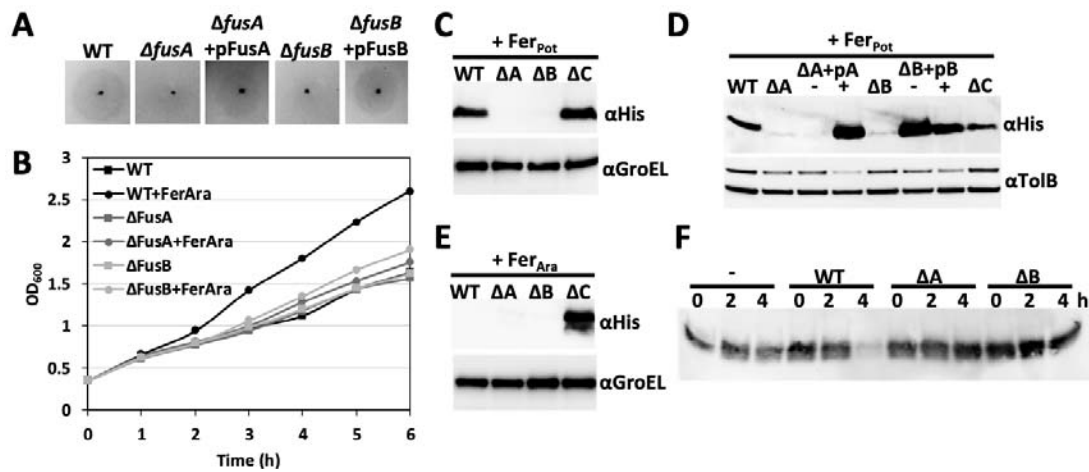


**Figure 2. *FusA* and *FusB* are required for ferredoxin uptake.** (A) Growth enhancement assay using spinach ferredoxin spotted onto soft agar overlay containing wild-type (WT), deletion strains and deletion strains recomplemented with the respective plasmid. (B) Growth curve comparing the rate of growth of wild-type and each deletion strain in the absence and presence of Arabidopsis ferredoxin. (D) Internalisation assay of  $\text{Fer}_{\text{Pot}}$ ; mid-log phase cells of each strain were supplemented with 2,2'-bipyridine and 1  $\mu\text{M}$  ferredoxin, grown for 1 hour and whole cell extracts were probed with anti-His antiserum. (E) Internalisation assay of  $\text{Fer}_{\text{Pot}}$  including deletion strains recomplemented in *trans* using plasmids encoding the respective genes (“ $\Delta\text{A}+\text{pA}$ ” =  $\Delta fusA+\text{pFusA}$ , “ $\Delta\text{B}+\text{pB}$ ” =  $\Delta fusB+\text{pFusB}$ ); prior to the addition of 2,2'-bipyridine and ferredoxin, the cultures of recomplemented strains were split in two and either supplemented with 0.5mM IPTG (“+”) or grown in the absence of inducer (“-“). (F) Internalisation assay using  $\text{Fer}_{\text{Ara}}$  (see D). (G) Depletion assay showing the gradual reduction of Arabidopsis ferredoxin level in the media derived from uninoculated (-), wild-type,  $\Delta fusA$  ( $\Delta\text{A}$ ) and  $\Delta fusB$  ( $\Delta\text{B}$ ) cell cultures.

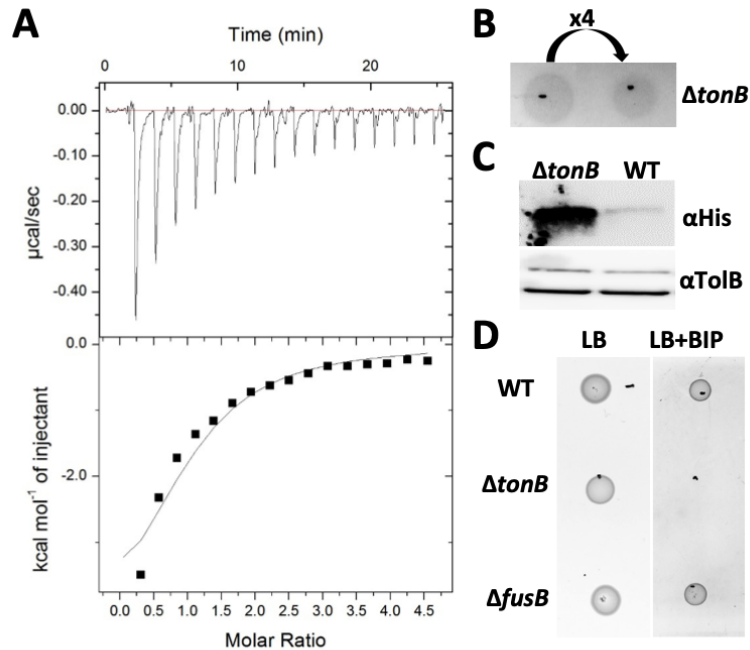


**Figure 3. FusB interacts with the FusA ‘TonB-box’ and ExbB, but not PcTonB, is required for ferredoxin uptake.** (A) ITC binding isotherm of 1 mM FusA<sub>NTR</sub>-GFP titrated into 90  $\mu\text{M}$  FusB<sub>CTD</sub>. The calculated  $K_d$  for the FusA<sub>NTR</sub>-GFP-FusB<sub>CTD</sub> complex is 57( $\pm$ 12)  $\mu\text{M}$  (n=3). (B) Growth enhancement assay using spinach ferredoxin on soft agar overlay containing  $\Delta\text{tonB}$  cells; x4 refers to dilution factor. (C) Uptake of potato ferredoxin by  $\Delta\text{tonB}$  and wild-type cells over the course of 1 hour. (D) Growth assay of wild type (WT),  $\Delta\text{tonB}$  and  $\Delta\text{fusB}$  cells spotted onto LB agar (LB) or LB agar supplemented with 400 $\mu\text{M}$  2,2'-bipyridine (LB+BIP).

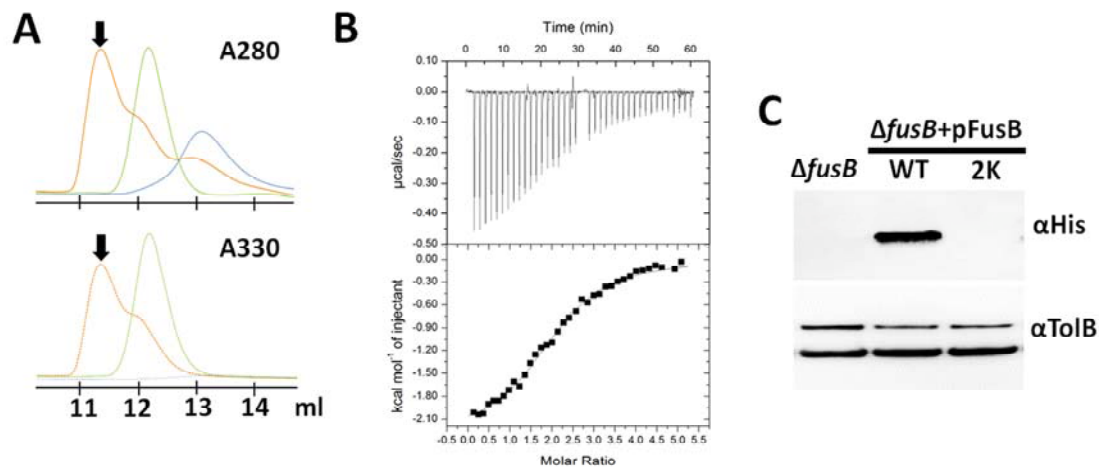


**Figure 4. FusB interacts with ferredoxin substrate.** (A) Overlaid size exclusion chromatograms of FusB<sub>CTD</sub> (blue), spinach ferredoxin (green) and a mixture of the two proteins (orange) with the arrow pointing at the ferredoxin-FusB<sub>CTD</sub> complex. (B) ITC binding isotherm of 600  $\mu\text{M}$  Fer<sub>Sp</sub> titrated into 70  $\mu\text{M}$  FusB<sub>CTD</sub>. The calculated  $K_d$  for the Fer<sub>Sp</sub>-FusB<sub>CTD</sub> complex is  $8.7(\pm 3.5)$   $\mu\text{M}$  ( $n=3$ ). (C) Ferredoxin import assay showing the level of potato ferredoxin uptake by  $\Delta\text{fusB}$  cells complemented with plasmids encoding either wild type (WT) or FusB<sub>CTD</sub> R176K/R177K (2K).

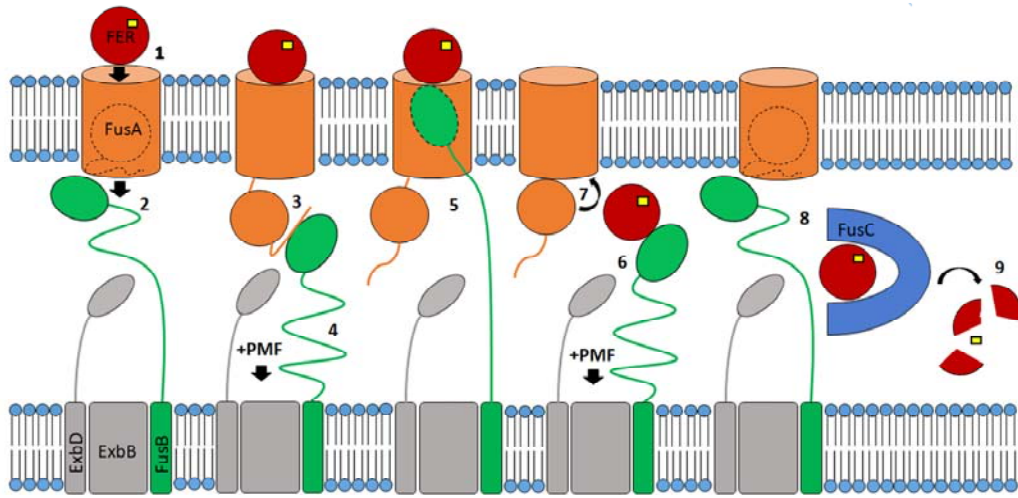


**Figure 5. Proposed mechanism of FUS-mediated ferredoxin import mechanism.** In the proposed mechanism FusB (green) fulfils two roles, firstly in displacement of the FusA plug domain and secondly in directly mediating ferredoxin translocation via the FusA lumen. Binding of ferredoxin (red) to FusA at the cell surface (1) causes release of the FusA TonB-box into the periplasm (2) where it is bound by FusB, which dislocates the plug domain (3) through energy transduced from the PMF via the ExbBD complex (4). FusB is then able to enter the lumen of FusA, bind ferredoxin (5) and through transduction of the PMF, translocate ferredoxin into the periplasm (6). The plug domain is then able to re-enter the FusA barrel (7) and return the FusA and FusB proteins to their resting states. Ferredoxin is then bound by FusC in the periplasm (8), which proteolytically cleaves the substrate releasing the iron-sulphur cluster (yellow) (9).

## Supplementary Information

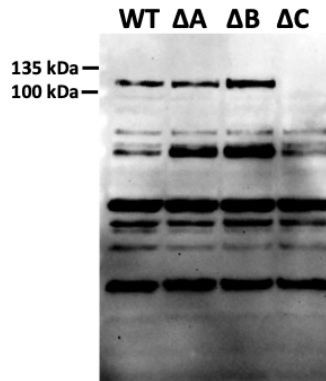


**Figure S1. FusC is produced in  $\Delta fusA$  and  $\Delta fusB$  strains.** Immunoblot showing the level of FusC (101 kDa) in the periplasmic fractions extracted from wild-type,  $\Delta fusA$  ( $\Delta A$ ),  $\Delta fusB$  ( $\Delta B$ ) and  $\Delta fusC$  ( $\Delta C$ ) cells grown to mid-log phase in the presence of 2,2'-bipyridine.

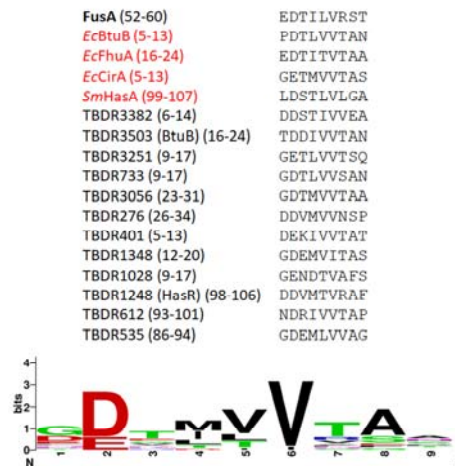


**Figure S2. Sequence alignment of the putative TonB box regions of FusA against other Pc LMG2410 and *E. coli* TonB box regions.** The numbers refer to the position of the predicted TonB box in the mature protein. Three Pc LMG2410 proteins were not included as their TonB boxes were not clearly identifiable. Sm refers to *Serratia marcescens*, Ec to *E. coli*. The consensus sequence shown below was generated using Weblogo.

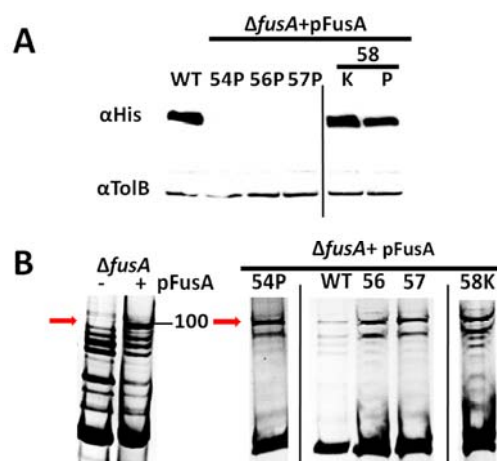


**Figure S3. Mutations within the putative FusA TonB box affect ferredoxin transport.** A – potato ferredoxin import assay of  $\Delta fusA$  cells reconstituted with gene encoding either wild type or FusA variants. B – outer membrane extracts confirming the expression and appropriate localisation of wild type and mutant FusA.

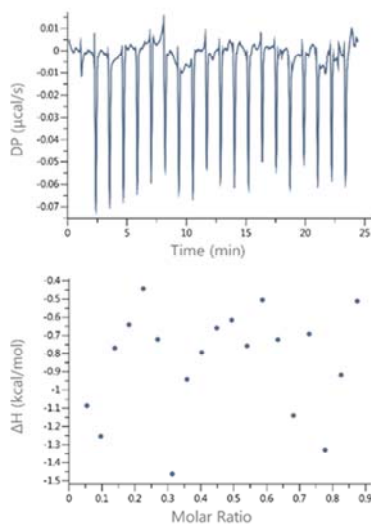


**Figure S4. GFP does not interact with FusB<sub>CTD</sub>.** Titration of 1.2 mM GFP, resulting from TEV mediated cleavage of FusA<sub>NTR</sub>-GFP, into 60  $\mu M$  FusB<sub>CTD</sub>.

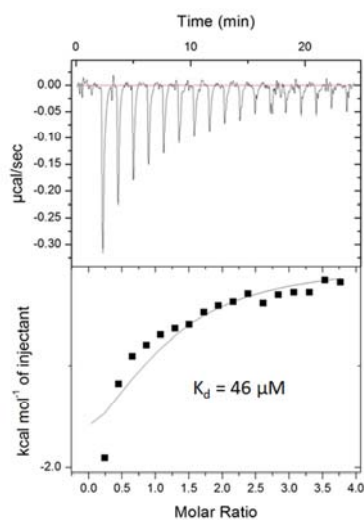


**Figure S5. TonB<sub>CTD</sub> forms a complex with the N-terminal domain of FusA.** ITC was performed by titrating 1.2 mM FusA<sub>NTR</sub>-GFP into 45  $\mu\text{M}$  TonB<sub>CTD</sub>.

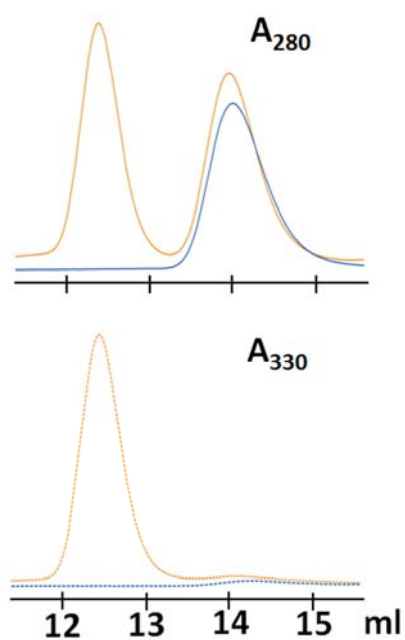


**Figure S6. TonB<sub>CTD</sub> does not form a complex with ferredoxin.** Overlay of size-exclusion chromatograms showing TonB<sub>CTD</sub> in the absence (blue trace) and in the presence of Fer<sub>SP</sub> (orange trace).



```

FusB      AARGAGKSN-SQNFRALHRRVN-YPSRAKALGVEGKVRVKFDITGSGTNTNVQVLSETPD
EcTonB    AATSKPVTSVASGPRALSRNQFPYPARAQALRIEGQVKVKFDVTPDGRVDNVQLLSAKPA
PcTonB    AASTQ-----SSGPRPLSRAQPQYPARAFSLRVEGRVKMQFDVDESGRVDNVRLSAEPR
          **          :.. *.* *   **:* * : * :*. :. :* * : * * * : * *
          **          :.. *.* *   **:* * : * :*. :. :* * : * * * : * *
          ▲ ▲ ▲
FusB      GVFGDDVVKDMARWRRTAPVENQVVSIVFKLNHGRVDDQQ
EcTonB    NMFEREVKNAMRRWRYEPGKPGSGIVVNILFKINGTTEIQ---
PcTonB    NMFERDIKAMRKWRYEAGKPGKDLVVTIVFKIDGGAAVE---
          . : *   : : * . * * * . * .. ** . * : * : * : * : * : :
    
```

**Figure S7. ClustalW sequence alignment of the C-terminal domains of FusB, PcTonB and EcTonB.** Alignments start at residue 211 of FusB, 158 of PcTonB and 140 of EcTonB. Black arrows indicate the highly conserved Tyr and Pro residues, red ones show arginines in FusB that are present in the first loop of the C-terminal domain.

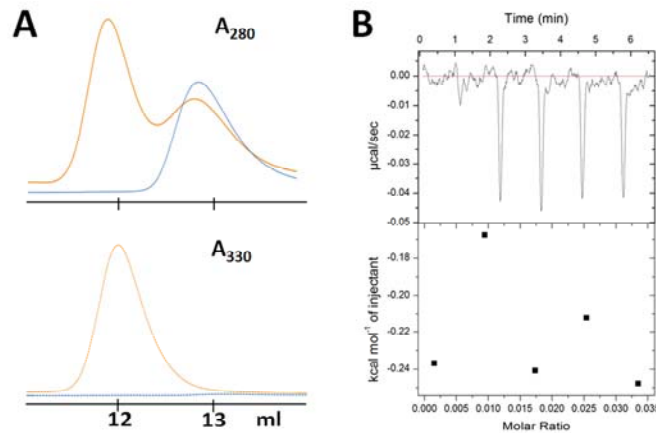


**Figure S8. Substitution of two arginine residues in FusB<sub>CTD</sub> with two lysines precludes interaction with ferredoxin molecule.** A – size exclusion chromatograms at 280 and 330nm of FusB<sub>CTD</sub>2K alone (blue) or in the presence of spinach ferredoxin (orange) showing no complex formation. B – ITC titration of Fer<sub>Sp</sub> into FusB<sub>CTD</sub>2K showing only heats of dilution.

**Table S1. List of primers used in this study.**

Target plasmid/ gene	Primer name	Primer sequence (5'→3')
fusA knockout	FusAKOfor	CACATGGAATTTACAATAATATTTTATTTTTAAAATGAT TATGCGTGTAGGCTGGAGCTGCTTC
	FusAKOrev	GGATTTACCAGGTGTAAGCGACGCCAAGCCAGAACT GACGGCCCATATGAATATCCTCCTTAG
fusB knockout	FusBKOfor	CTGCACTACTGACACCAGGAAGTTGAAGTTTAAGAG ATGGAGTTGGGTGTAGGCTGGAGCTGCTTC
	FusBKOrev	CCCAATAAGCATAATCATTTTAAAATAAAAATATTATT GTAAATTCCCATATGAATATCCTCCTTAG
TonB knockout	TonBKOfor	CGTGATGTTGTTTGAAGACAATAGTGCAGGACAATA GGTTGGTGTAGGCTGGAGCTGCTTC
	TonBKOrev	CGCGCTCGAACATATTGCGTGGCTCAGCAGAAAGCA CGCGCACGCATATGAATATCCTCCTTAG
ExbB knockout	ExbBKOfor	GTACAGAACAGATGATTGTACAGAACGAATGGTGG GGCACAGCGTGTAGGCTGGAGCTGCTTC
	ExbBKOrev	CGTTGCTGGCAGCCACATCGAGATCGCGACTTTGCA GCAGCAGCATATGAATATCCTCCTTAG
pFusA	FusAfor	GGAATTCCATATGAATAAGAACGTCTATTTAATG
	FusA rev	CAGCTCGAGTTACCAGGTGTAAGCGAC
pFusB	FusBfor	GGAATTCCATATGAGTAGTGAAAATCTTC
	FusBrev	CTGCTCGAGTTATTGCTGGTCATCAAC
pFusB-CTD	FusBCTDfor	GGAATTCCATATGGCGGCAACGGCCAAGG
	FusBCTDrev	CACCTCGAGTTGCTGGTCATCAAC
pTonB-CTD	TonBCTDfor	GGAATTCCATATGGCAGCAAGCACGCAGTC
	TonBCTDrev	CACCTCGAGTTGACTGCCGCCCCGCC
pExbB	ExbBfor	GGAATTCCATATGAAGACGGCTGTCAGTAATAC
	ExbBrev	CACCTCGAGTTAACCCACCCGCAGTTTATG
pFusANTR-GFP	FusANTRfor	GAGCTCGAGATGCAGCAAAATGATACCTCTG
	FusANTRrev	CACGGATCCCATCGACTGACTAGTCGGGG
pFusA-E49P	FusAE49Pfor	GTGATTCCTCTTCGCCGAACGGCGAAGATAC
	FusAE49Pprev	GTATCTTCGCCGTTTCGGCGAAGAGGAATCAC

pFusA-E52P	FusAE52Pfor	CTTCGGAAAACGGCCCGGATACGATTTTAGTC
	FusAE52Prev	GACTAAAATCGTATCCGGGCCGTTTTCCGAAG

**Table S2. List of plasmids used in this study**

Plasmid name	Vector backbone	Source
pKD4	pANTSy	Datsenko & Wanner 2000
pKD46	pINT-ts	Datsenko & Wanner 2000
FusA <sub>NTR</sub> -GFP	pWaldo (Waldo et al 1999)	This study
pFusA	pJ404	This study
pFusB	pJ404	This study
pFusC	pJ404	Mosbahi et al 2018
pFusB-CTD	pJ404	This study
pTonB-CTD	pJ404	This study
pExbB	pJ404	This study
pFerAra	pET21	Grinter et al 2016
pFerPot	pET21	Grinter et al 2016